Electronic Supplementary Material (ESI) for Physical Chemistry Chemical Physics.

Probing the mechanisms of enhanced crystallisation of APS in the presence of Ultrasound

Peter R. Birkin, Jack J. Youngs, Tadd T. Truscott and Silvana Martini

Figure S1 shows the timings used in the crystallisation experiments.

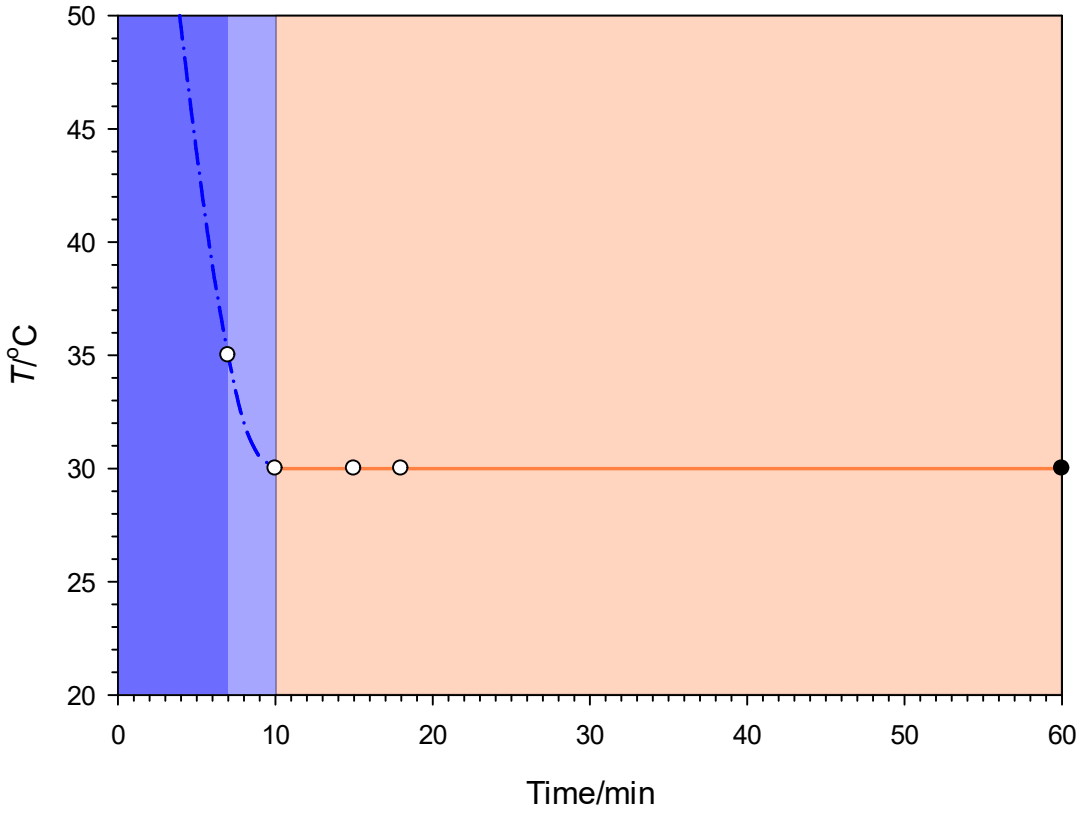

Figure S1. Schematic representation of the timings and temperature of the APS sample during the cooling/crystallisation experiments. The cooling of the sample ( ) is aided by mechanical stirring of the sample (note the stirring stops at 7 min for that particular experiment). An estimate (based on manual inspection of the cooling profile with a digital thermometer) of the cooling profile is shown (— • —). HIU (75 W, 10 s) was applied at different times (○) during the experiment. Microscope images were recorded at different times (○, ●) through the entire experiment.

The terminal velocity of bubbles is a rather complex topic with a number of factors to consider[1–4]. The size of the gas bubble as well as the degree of advantageous materials at the surface can alter the velocity quite considerably. The terminal velocity (v) of a bubble can be given by equation (1). Note here we assume an approximate form for the size range of interest in the oil systems and that the interface is clean[5] and free of nanocrystalline TAG[6] molecules.

$$v = \frac{gr^2(\rho_l - \rho_g)}{3\eta} \quad (1).$$

where g is acceleration due to gravity (9.81 m s^{-2}), r is the bubble radius (m), ρ_l and ρ_g the density of the fluid and gas respectively (kg m^{-3}) and η the viscosity of the fluid (kg m^{-1} s^{-1}). Using the measured viscosities of APS, figure S2 (a) shows the terminal velocity of bubbles as a function of size while figure S3 shows the effect of temperature on the terminal velocity of a 100 µm radius bubble as a function of temperature (which in turn changes the viscosity).

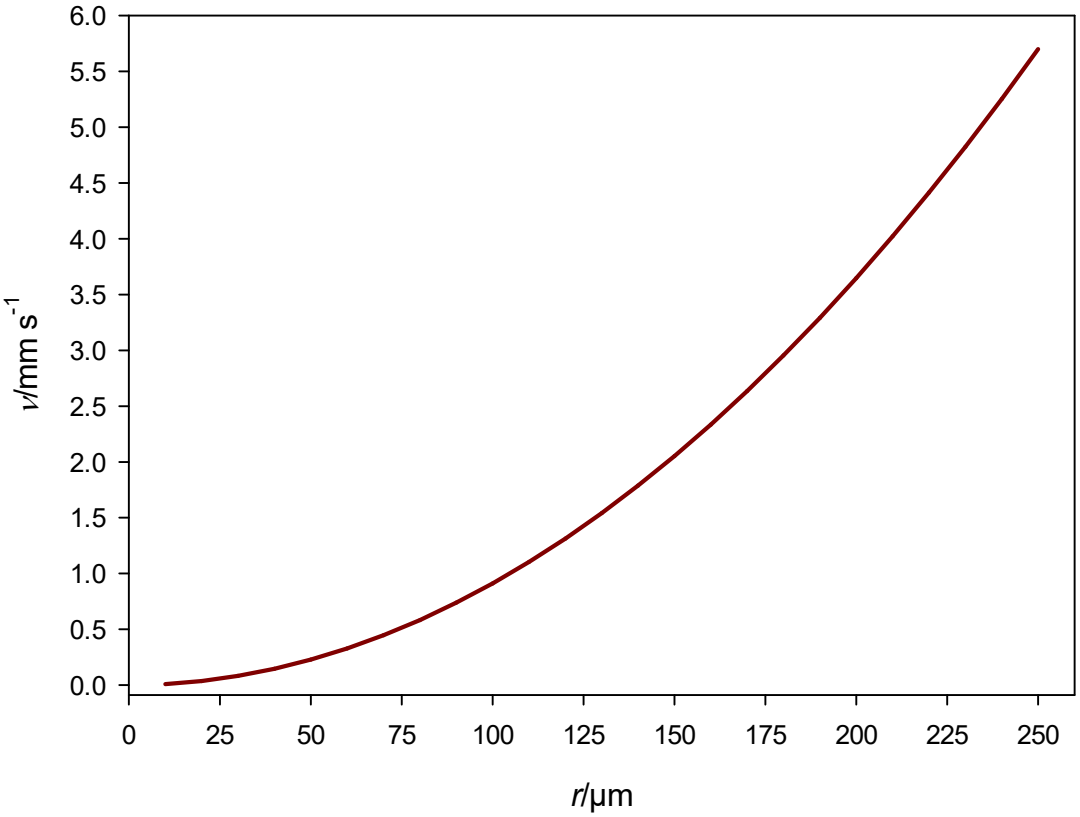

Figure S2. Plot showing the calculated terminal velocity of a nitrogen gas bubble as a function of size by applying equation (1). Here the viscosity at 30°C (0.03291 kg m^{-1} s^{-1}) is used along with an assumed density of the fluid of 919 kg m^{-3} and the gas 1.12 kg m^{-3}. Here atmospheric pressure is assumed to be 101 kPa.

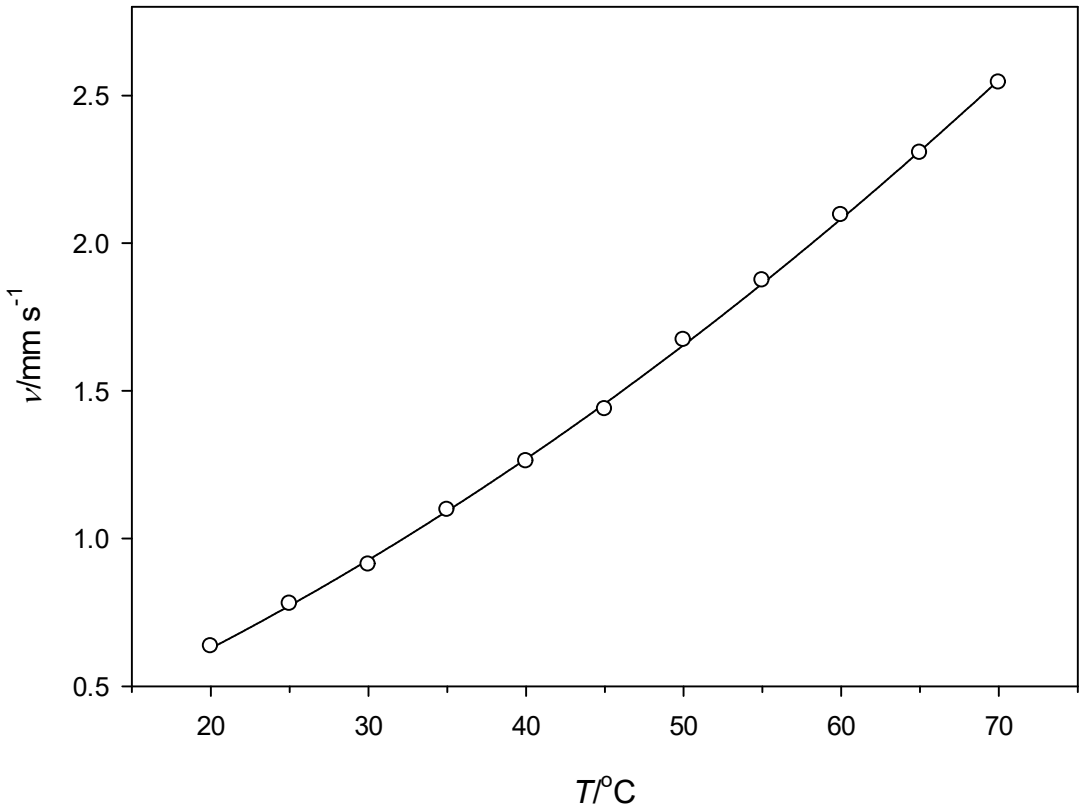

Figure S3. Plot showing the calculated terminal velocity (○) of a 100 µm radius nitrogen gas bubble as a function of temperature by applying equation (1). Here the viscosity of APS was employed at each temperature along with an assumed density of the fluid[7] of 919 kg m^{-3}. Here atmospheric pressure is assumed to be 101 kPa. The trend line is added for a visual aid only.

To calculate the time taken for a nitrogen gas bubble to dissolve in APS, the approach developed by Epstein and Plesset was adopted[8]. Under this assumption, for nitrogen saturated media, the dissolution time can be calculated using equation (2).

$$t_{dis} = \frac{R_0^2(1+\delta)}{3\kappa D\delta} \quad (2)$$

Here, δ and τ are defined as follows.

$$\delta = \frac{\tau}{R_0\rho_g}$$

$$\tau = \frac{2m\gamma}{RT}$$

where R_0 is the initial bubble size (m), κ is the Ostwald constant[9] for the gas in the media (0.07 for oil, 0.016 for water), m is the molecular mass of nitrogen (0.028 kg mol^{-1}), γ is the surface tension (assumed[7] to be 0.0327 N m^{-1} for oil. 0.072 N m^{-1} for water), R is the gas constant (8.314 J K^{-1} mol^{-1}),

D the diffusion coefficient of molecular nitrogen in oil (4.7 x 10^{-11} m^2 s^{-1}) ρ_g is the density of nitrogen inside the bubble in the absence of surface tension effects (1.15 kg m^{-3}) and T the temperature (295 K). Note the values are taken for food oils under similar conditions. The diffusion coefficient of N_2 in APS is calculated assuming a value[10] in water of 2.2 x 10^{-9} m^2 s^{-1} at 295 K and applying the Stokes Einstein relationship[11]. Here we assume that the hydrodynamic radius is the same in both media. Exact values for some of these parameters are unknown hence, the values stated are for other food oils in this case and can be found in the referenced literature.

Figure S4 shows the dissolution rate in oil compared to water.

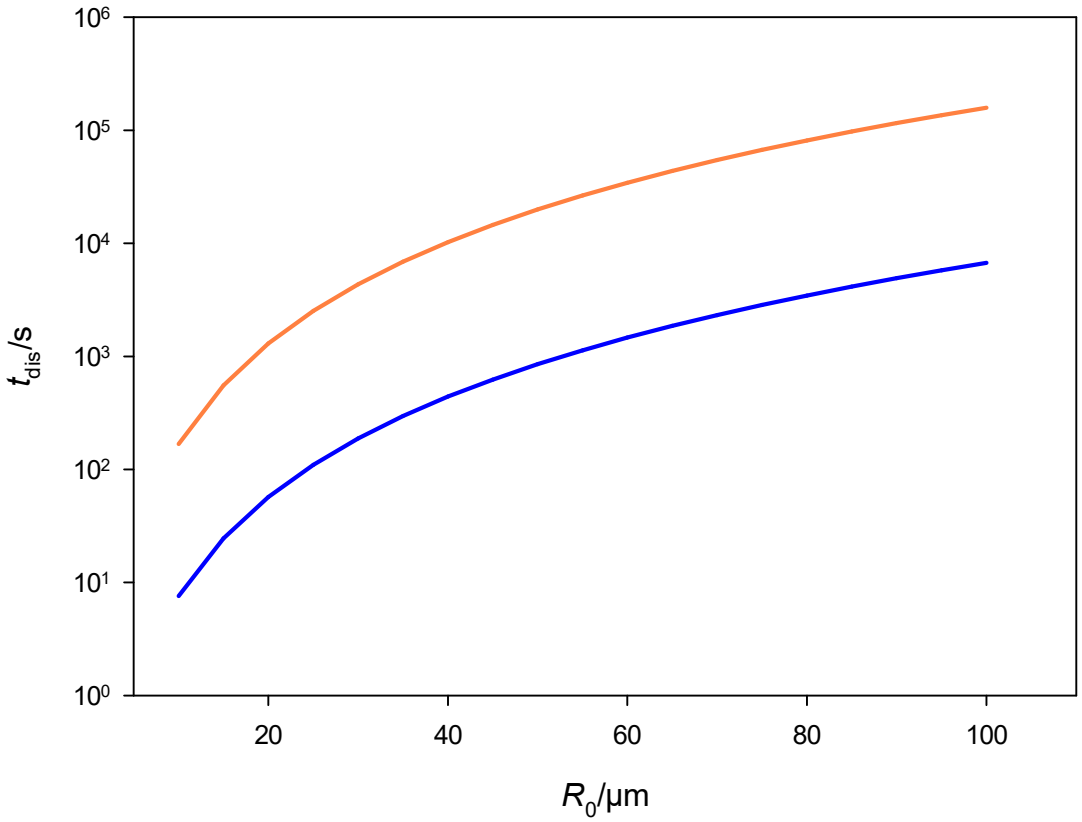

Figure S4. Plot showing the estimated dissolution time apply the theory developed by Epstein and Plesset to nitrogen bubbles as a function of the initial bubble size. The plot shows the values for oil (—) and water (—) for comparison. Both curves were calculated at 295 K.

Figure S5 shows the material characteristics of the samples treated with/without ultrasound and with additions of crystals to the media.

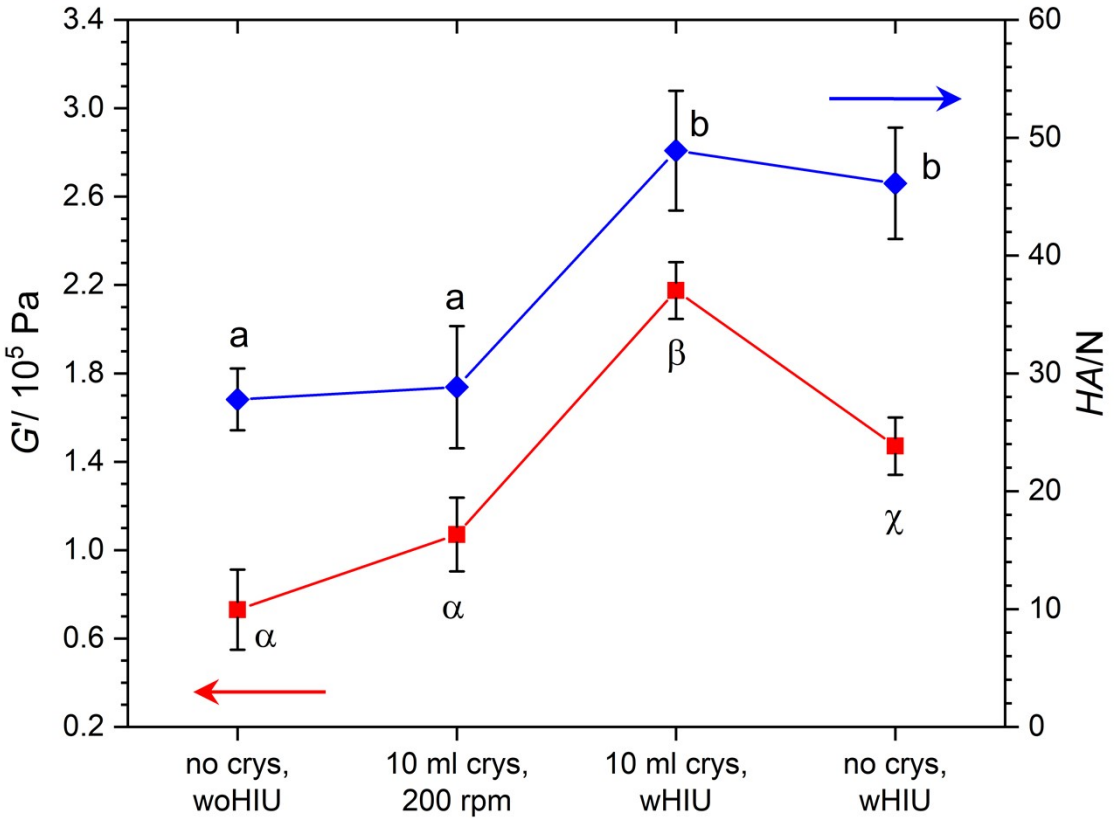

Figure S5. Plots showing elastic modulus (G', —)) and hardness (HA, —)) measurements recorded for APS crystallised in presence of pre-crystallised APS material (10 ml crys) and with(w) or without(wo) HIU treatment. For non-sonicated samples agitation (200 rpm) was employed to briefly combine the added crystalline material with existing APS sample. Values are recorded from three repeat crystallisation experiments and expressed as mean ±95 % CL. Values labelled with different superscript lettering indicate significant differences ($p < 0.05$).

Figure S6 shows the corresponding PLM images.

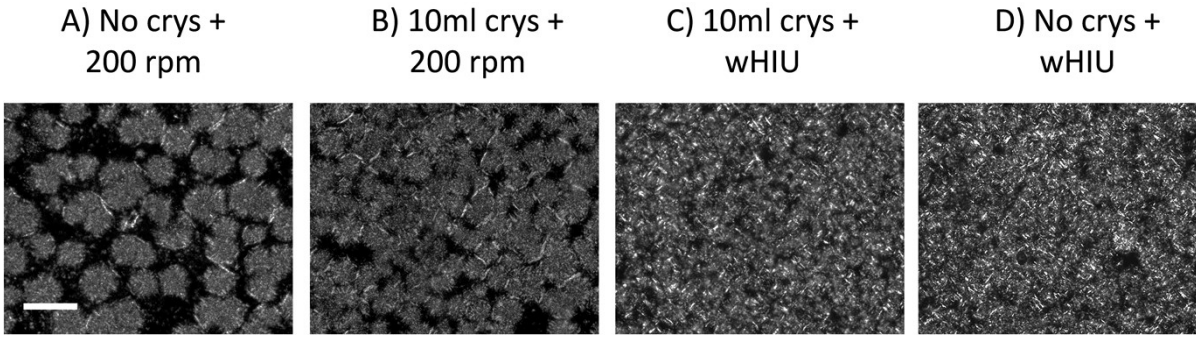

Figure S6. Crystal microstructure of all-purpose shortening (APS) crystallised in the presence of pre-crystallised APS material (10 ml crys) and with(w) or without(wo) HIU treatment. For the non-sonicated sample agitation (200 rpm) was employed to briefly combine the added crystalline material with existing APS sample. The scale bar represents 100 µm.

References

1 N. P. Brandon, Imperial College, 1985.

2 N. P. Brandon and G. H. Kelsall, Growth kinetics of bubbles electrogenerated at microelectrodes, *J. Appl. Electrochem.*, 1985, **15**, 475–484.

3 G. H. Kelsall, S. Tang, A. L. Smith and S. Yurdakul, Measurement of rise and electrophoretic velocities of gas bubbles, *J. Chem. Soc. Faraday Trans.*, 1996, **92**, 3879.

4 R. Clift, J. R. Grace and M. E. Weber, *Bubbles, Drops, and Particles*, Dover Publications Inc., New York, 2005.

5 M. A. Borden and M. L. Longo, Dissolution Behavior of Lipid Monolayer-Coated , Air-Filled Microbubbles : Effect of Lipid Hydrophobic Chain Length, *Langmuir*, 2002, **18**, 9225–9233.

6 N. C. Acevedo, F. Peyronel and A. G. Marangoni, Nanoscale structure intercrystalline interactions in fat crystal networks, *Curr. Opin. Colloid Interface Sci.*, 2011, **16**, 374–383.

7 W. Duangsuwan and U. Tuzun, The Dynamics of Single Air Bubbles and Alcohol Drops in Sunflower Oil at Various Temperatures, *AIChE J.*, 2011, **57**, 897–910.

8 P. S. Epstein and M. S. Plesset, On the Stability of Gas Bubbles in Liquid-Gas Solutions, *J. Phys. Chem.*, 1950, **18**, 1505–1509.

9 R. Battino, T. R. Rettich and T. Tominaga, The Solubility of Nitrogen and Air in Liquids, *J. Phys. Chem. Ref. Data*, 1984, **13**, 563.

10 P. T. H. M. Verhallen, L. J. P. Oomen, A. J. J. M. v. d. Elsen, J. Kruger and J. M. H. Fortuin, The diffusion coefficients of helium, hydrogen, oxygen and nitrogen in water determined from the permeability of a stagnant liquid layer in the quasi-s, *Chem. Eng. Sci.*, 1984, **39**, 1535–1541.

11 P. W. Atkins, *Physical Chemistry*, Oxford University Press, Oxford, 1986.